Polymer/Laponite Nanocomposite Films Produced from Surfactant-Free Latexes using Cationic macroRAFT Copolymers

Thaíssa C Chaparro, Rodrigo D Silva, Franck D'agosto, Muriel Lansalot, Florent Dalmas, Laurent Chazeau, Amilton M Santos, Elodie Bourgeat-Lami

Polymer/Laponite® nanocomposite films produced from surfactant-free latexes using cationic macroRAFT copolymers

Thaíssa C. Chaparro[a,b], Rodrigo D. Silva[a], Franck D'Agosto[b], Muriel Lansalot[b], Florent Dalmas[c], Laurent Chazeau[c], Amilton M. Santos[a*], Elodie Bourgeat-Lami[b]*

[a]Engineering School of Lorena – University of São Paulo, 12.602-810 Lorena/SP, Brazil.
[b]Univ Lyon, University Claude Bernard Lyon 1, CPE Lyon, CNRS, UMR 5128, CP2M (Catalysis, Polymerization, Processes and Materials), 43, Blvd du 11 Novembre 1918, F-69616 Villeurbanne, France.
[c]Université de Lyon, INSA-Lyon, CNRS MATEIS UMR5510, 7 av J. Capelle, F-69621 Villeurbanne, France
[*]Email: amsantos@usp.br,
[*]Email: elodie.bourgeat-lami@univ-lyon1.fr

Abstract.

In this work, the use of positively charged macromolecular reversible addition-fragmentation chain transfer (RAFT) copolymers (macroRAFTs) in the synthesis of Laponite® RD-based nanocomposite latex particles is described. For this purpose, two different amphiphilic copolymers composed of 2-(dimethylamino)ethyl methacrylate (DMAEMA) and *n*-butyl acrylate (BA) units are investigated. In a first step, the macroRAFT is adsorbed onto Laponite® and then in a second step, the macroRAFT-modified clay platelets are used in the emulsion polymerization of methyl methacrylate (MMA), methyl acrylate (MA) or styrene (Sty), with BA. By acting as both coupling agents and stabilizers, the macroRAFT agents lead to the formation of partially encapsulated particles and dumbbell structures. When hydrophobic monomer mixtures that can form film are used, these morphologies result in nanocomposite films with increased stiffness, in comparison to the pure polymer matrix. As observed by dynamic mechanical analysis, the high Young's modulus level presented by the composite films in the rubbery plateau (above 100 MPa when filled with 10 wt% of clay) highlights the strong mechanical reinforcement. Such improvement can be attributed to the formation of two percolating networks – one of homogeneously distributed and connected platelets and one of macroRAFT chains – within the polymer matrix.

1. Introduction

The incorporation of clays such as layered silicate nanoparticles into polymer matrices has attracted great attention in the recent literature.[1-4] Among the many benefits of these nanocomposites, one can cite improved barrier properties, mechanical strength, thermal stability and fire retardancy.[5-7] The possibility of alignment of these high aspect ratio particles into the polymeric matrix is another factor that make these materials very attractive. [8] Among the methods for the preparation of nanocomposites, heterogeneous polymerization techniques in aqueous media are particularly interesting since they allow the design of colloidal nanocomposites with controlled morphology that can further be processed in materials with tailored properties.[9-11] Moreover, the use of water as dispersion medium allows adequate conditions for the exfoliation of layered silicates[7] making them suitable to be used in process such as emulsion and miniemulsion polymerization.[12-14] Both techniques have proven to be potential tools to prepare polymer/inorganic particles and highly suitable to generate a wide variety of composite colloidal particles.[15-17] An interesting morphology that has been achieved by surfactant-free emulsion polymerization is the so-called armored morphology in which polymer particles are covered with Laponite® platelets.[13, 18-20] These latexes can be used to prepare nanostructured polymer films with platelets orderly distributed, forming a honeycomb-like structure that results in enhanced mechanical properties.[18] The resulting colloidal nanocomposites from such processes can be easily handled and be used in practical and interesting industrial applications such as adhesives and coatings.[21, 22]

A particular strategy that has emerged and revealed to be very versatile for the preparation of nanocomposite particles in aqueous dispersed media combines emulsion polymerization and reversible addition-fragmentation chain transfer (RAFT).[23, 24] Coined macroRAFT-assisted encapsulating emulsion polymerization (REEP), this method relies on the use of RAFT homopolymers or copolymers (macroRAFT agents) that can direct the growth of the polymer

chains on the surface of the particles, restricting it (preferably) to the inorganic substrate. In addition, macroRAFT agents can act as stabilizers, discarding, in most cases, the need for additional surfactant. The encapsulation of inorganic particles with a layer of binder polymer yielding core-shell hybrid particles has shown to be of great interest in the last few years as it is an ultimate solution to avoid agglomeration of the inorganic objects and guarantee that they remain isolated during the film formation process, besides offering the possibility to control their arrangement in the nanocomposite film.[25] Since the invention of this strategy by Hawkett's research group,[26] a variety of inorganic nanoparticles has been encapsulated, mostly spherical.[27-33] Although the encapsulation of high aspect ratio inorganic particles by emulsion polymerization approaches is known to be more challenging due the high surface energy of these systems,[34] there are also examples in literature of the encapsulation by REEP of non-spherical particles such as Gibbsite platelets,[35] carbon nanotubes,[36, 37] graphene oxide nanosheets,[38] layered double hydroxides (LDHs)[39, 40] and Montmorillonite (MMT) platelets.[41] Nanocomposite particles with morphologies other than core-shell have also been prepared by means of the REEP process. Guimaraes et al.[42] synthesized Laponite®-armored latexes using a linear poly(ethylene glycol) (PEG)-based macroRAFT agent. In this case, the morphology arose from the co-assembly and/or heterocoagulation events between nano-objects formed in the aqueous phase from chain extension of free (non-adsorbed) macroRAFT agents and chain-extended macroRAFT agent-adsorbed clay platelets. Pearson et al.[40] prepared polymer/LDHs nanoparticles with sandwich and armored morphology using RAFT copolymers bearing acrylic acid (AA) and *n*-butyl acrylate (BA) units (P(AA-*co*-BA)). The sandwich morphology was achieved using a P(AA-*co*-BA) macroRAFT agent with relatively high molar mass (shorter ones giving rise to encapsulated hybrid particles as mentioned ahead), while the armored particles were achieved by removing the thiothiocarbonylated chain end from P(AA-*co*-BA) prior to its adsorption on LDHs. In this work, the morphology was correlated to the density of thiothiocarbonylated chain ends on the inorganic surface. Silva et al.[43, 44] prepared

polymer-decorated MMT platelets using macroRAFT agents composed of AA, BA and poly(ethylene glycol) methyl ether acrylate (PEGA) units. In this case, morphology as well as latex stability were influenced by the nature, molar mass and degree of ionization of macroRAFT agents. Chaparro et al.[45] prepared polymer/Laponite® latexes with Janus and dumbbell morphologies which could be correlated to factors such as the fraction of free macroRAFT agent at the beginning of polymerization, the affinity between macroRAFT agent and clay and the adequate hydrophilic–hydrophobic balance within the macroRAFT structure. The use of PAA-*b*-PPEGA block copolymer as macroRAFT agent generated mainly Janus composite particles. When the more hydrophobic PAA-*b*-P(PEGA-*co*-BA) macroRAFT agent was employed, the production of particles with a dumbbell morphology was favored. Dumbbell and Janus morphologies were also achieved by using P(PEGA-*co*-BA) and P(AA-*co*-BA) to mediate the polymerizations, but a better wetting of the clay surface was achieved with the latter, which resulted in flat Janus and sandwiched hybrid particles.

Although many works described successful application of the REEP process, most do not progress towards film-forming studies mainly because the encapsulated morphology, achieved for polymers with relatively high glass transition temperature (T_g), normally cannot be kept when a comonomer mixture yielding polymers with T_g lower than the reaction temperature is used.[34] During the encapsulation of (hydrophilic) inorganic nanoparticles with a (hydrophobic) polymer shell, the nanoparticles tend to exclude themselves, searching the polymer/water interface so a state of minimal interfacial energy can be achieved. Thus, several parameters, related especially to kinetics and/or thermodynamic control mechanisms, must be optimized. Some strategies that have been used to keep the encapsulated morphology includes the use of a cross-linking agent to restrict the mobility of the polymer chains around the particles, trapping the latter inside the polymer shell.[40] However, this approach prevented further film formation. Another one includes forming a hard polymer shell around the inorganic nanoparticles followed by the formation of a second soft shell to enable film

formation.[43] Interestingly, Pearson et al.[40] encapsulated LDHs platelets with a low T_g copolymer composed of methyl methacrylate (MMA) and methyl acrylate (MA) using low molar mass P(AA-*co*-BA) macroRAFT agent which was ascribed to the higher density of thiothiocarbonylated chain ends that promoted more efficient polymer growth on LDH surface. The resulting hybrid latexes were subsequently processed to LDHs-filled nanocomposites with a microstructure consisting of a percolating P(AA-*co*-BA)-LDH phase and isolated LDH particles within a soft polymer matrix, giving rise to strong mechanical reinforcement.[46]

Even though the number of studies involving the REEP process and different inorganic objects has increased in the last years, there are very few works on Laponite® clay.[42, 45] In addition, the use of cationic macroRAFT agents has not been investigated in these works although it has proven to be effective for MMT encapsulation.[44, 47] This type of macroRAFT agent should be particularly interesting to enable the preparation of polymer/Laponite® colloidal particles with different morphologies. In that context, the focus of this work was to evaluate the effectiveness of the REEP strategy for the synthesis of anisotropic composite latex particles incorporating Laponite® platelets using amphiphilic 2-(dimethylamino)ethyl methacrylate (DMAEMA)-based macroRAFT copolymers. Initially, the macroRAFT agents were designed and synthesized by solution polymerization and the adsorption of these molecules onto Laponite® was then performed in aqueous medium and studied by adsorption isotherms, as described previously in the literature.[48] Emulsion polymerization of MMA, MA or styrene, with BA was then carried out in the presence of the macroRAFT agent-modified clays to generate clay/polymer nanocomposite latex particles under semi-batch conditions and in the absence of surfactant. Films were then characterized in terms of their microstructure by imaging a 2D cross-section of the material via focused ion beam-scanning electron microscopy (FIB-SEM). Finally, their mechanical properties were assessed by dynamic mechanical analysis (DMA) and correlated to film microstructure.

2. Experimental Section

2.1. Materials

Two macroRAFT agents with different hydrophilic-lipophilic balance and molar mass were used in this work, as listed in **Table 1**. They have been synthesized, submitted to a quaternization process, purified and characterized as described previously.[48] Laponite® RD particles were supplied by BYK Additives Ltd (former Rockwood Additives Ltd). This nanoclay was chosen among the layered silicates since it is an ideal model substrate, presenting a high chemical purity, a uniform dispersity in terms of size of the elementary platelets, which are disposed as disc-shaped crystals with a diameter of ~30 nm and thickness of ~ 0.92 nm when dispersed in water, and the ability to produce clear dispersions. Hydrochloric acid (HCl 1N, standard, Acros Organics) and the initiators azobis(2-methylpropionamide) dihydrochloride (AIBA, 98%, Acros Organics) and 2,2'-azobis[2-(2-imidazolin-2-yl)propane] dihydrochloride (ADIBA, 99%, Wako) were all used as received. The monomers: MMA (99%, Sigma-Aldrich), styrene (99% Sigma-Aldrich), BA (99%, Sigma-Aldrich) and MA (99%, stabilized, Acros Organics) were used without further purification.

Table 1. Overall monomer conversion (X), experimental molar mass ($M_{n,\,exp}$) and dispersity ($Đ$) of the macroRAFT agents used in this work.[48]

Entry	MacroRAFT agent	X [a] [%]	*nBA* [b]	*nDMAEMA* [b]	$M_{n,\,exp}$ [g mol^{-1}]	$Đ$
MR1	P(DMAEMA$_{10}$-*co*-BA$_4$)-TTC	86.6	3.9	9.7	1630	1.42
MR2	P(DMAEMA$_{19}$-*co*-BA$_{14}$)-TTC	81.1	14.2	18.5	4520	1.45

[a] *D*etermined by proton nuclear magnetic resonance (^{1}H NMR); [b] n = actual number of repeat units in the polymer chain based on the individual conversion of each comonomer, determined by ^{1}H NMR.[48]

2.2. Methods

Hybrid polymer/Laponite® latexes were synthesized in the presence of macroRAFT agents using a semi-continuous process. In a typical run, 0.125 g of Laponite® were added into a flask containing 10 mL of water. The dispersion was left under vigorous stirring for 30 minutes while, in parallel, the required amount of macroRAFT agent to achieve a final concentration of 2.2 mM (unless stated otherwise) was added into a flask and 10 mL of water were used to dissolve the polymer. In some cases, HCl were added for pH adjustment. In order to avoid stability issues related to neutralization of the clay surface charges, the negatively charged Laponite® dispersion was added into the flask containing the positively charged macroRAFT agent solution and, if necessary, a second pH adjustment was made at this point. The Laponite®/macroRAFT agent suspension was left stirring for 60 minutes and transferred to a 50 mL three-neck round-bottom flask. A solution of the initiator, AIBA or ADIBA, was previously prepared by adding the required amount of initiator (typically 3 times less than the molar concentration of macroRAFT agent) to the necessary amount of water to complete a total volume of 22.6 mL and added to the suspension. The system was adapted to a reflux condenser, a stirring plate and purged with nitrogen for 30 minutes. The monomer mixture (typically MMA/BA 90/10 mol%) was purged in a separate flask, and 0.1 g of the mixture was added to the reaction medium. To start polymerization, the system was heated to 80 ºC and 2.4 mL of the monomer mixture were fed at a rate of 0.6 mL h^{-1} for 4 hours. The polymerization was left for 1 to 3 additional hours after the end of the monomer addition and samples were taken every hour for kinetic study. A typical recipe (entry R2, **Table 3**) and conditions used in the synthesis are shown in **Table 2**.

Table 2. Typical recipe (entry R2, **Table 3**) and conditions used in the synthesis of hybrid latexes by RAFT-mediated emulsion polymerization in the presence of cationic macroRAFT agents.

Reagents	**Quantity**
[Laponite®] (g L^{-1})	5
[macroRAFT agent]/[Initiator]	3

Monomer initial shot (mL)	0.1
Monomer added (mL)	2.4
Monomer addition rate (mL h^{-1})	0.6
Monomer mixture (MMA:BA, mol%)	90:10
Total volume (mL)	25
Temperature (°C)	80

2.3. Characterizations

Monomer conversion (*X*) was determined by gravimetric analysis. Calculation was made considering a semi-continuous process, taking into account that, at a given time, different amounts of monomers had been added into and taken from the reactor. The instantaneous monomer conversion was calculated based on the amount of monomer mixture fed to the reactor up to the sampling time while overall monomer conversion was calculated based on the total amount of monomer fed during the experiment (the procedure to calculate both conversions is detailed in Supporting Information). The hydrodynamic average particle diameter ($Z_{av.}$) and the size dispersity (*PdI*, the higher this value, the broader the size distribution) were determined by dynamic light scattering (DLS) in a NanoZetasizer Malvern instrument. Even though this technique is recommended for spherical particles, it can be used as a useful indicative tool for the non-spherical particles obtained in this work. Particle morphology was determined by cryogenic transmission electron microscopy (cryo-TEM) using a Philips CM120 transmission electron microscope (Centre Technologique des Microstructures (CTμ), platform of the Université Claude Bernard Lyon 1, Villeurbanne, France). A drop of the dilute suspension was deposited on a holey carbon-coated copper grid and, before introduction in the microscope, the excess of liquid was removed from the grid with filter paper. The grid was then immersed into a liquid ethane bath cooled with liquid nitrogen and positioned on the cryo-transfer holder, which kept the sample at −180 °C and guaranteed a low-temperature transfer to the microscope. Images of the frozen hydrated latex specimens were acquired at an accelerating voltage of 120 kV.

For the observation of the microstructure of the polymer/Laponite® nanocomposites films in a larger scale, samples were sectioned and observed using a dual column focused ion beam (FIB)–scanning electron microscope (SEM) ZEISS NVision40, with a Ga^{2+} ion beam accelerated at 30 kV. To guarantee the observation of the materials with minimum charging effects, high resolution and a good contrast between the phases, a bulk nanocomposite trapezoid, previously metalized with gold, was first milled at high current beam (4 nA), in order to allow an imaging of the shorter face by the electron beam up to at least a 15 μm depth. A final polishing of the observed surface was then carried out with a fine current beam (80 pA). The SEM images of the polished surface were recorded under low voltage conditions (2 kV) using an in-lens secondary electron (SE) detector.

The thermo-mechanical response of the material was evaluated through dynamic mechanical analysis (DMA). The measurements were performed in a homemade apparatus (MATEIS, INSA of Lyon, France) in torsion mode at a fixed frequency of 1 Hz from 150 K to 400 K with a heating rate of 1 K min^{-1}. All samples were dried before analysis and their dimensions were about 10 mm long, 3 mm wide and 0.6 mm thick. The variation of the storage (G') and the loss (G'') moduli of the complex shear modulus (G*) with temperature was measured, and the mechanical main relaxation temperature was defined as the temperature at the maximum of loss modulus (G'').

3. Results and Discussion

The DMAEMA-based macromolecules have been carefully designed to interact with Laponite® particles, mediate the radical emulsion polymerization in the presence of clay, by carrying a reactivatable thiocarbonylthio functionality, and stabilize the growing hybrid particles. The study of their synthesis and ability to interact with the Laponite® surface has been reported in our previous work.[48] We have demonstrated that, upon adsorption of cationic macroRAFT agent onto the Laponite® surface, the number of clay negative charges decreases,

resulting in a substantial decrease of the absolute value of zeta potential and a concomitant increase in the particle size, indicating clay aggregation. As the macroRAFT concentration further increases, the particles undergo charge reversal (i.e. the sign of the zeta potential changes from negative to positive), and their size decreases as they become saturated with polymer, yielding colloidally stable and positively charged macroRAFT agent-adsorbed Laponite® platelets. Based on these previous results, we now wish to evaluate the role of adsorbed macroRAFT in stabilizing and controlling the morphology of Laponite®-based nanocomposite latexes via the REEP method. The syntheses of the nanocomposite latexes were carried out following the typical recipe shown in **Table 2**, but some parameters were varied in order to gain better insight into the process and will be specified when needed.

3.1. Effect of macroRAFT agent type and concentration

First, the influence of the macroRAFT agent nature on particle morphology and latex stability was evaluated, by comparing two different macroRAFT structures with different compositions, using initially a non-film-forming mixture of monomers (MMA:BA = 90:10 mol%). In addition, the as-synthesized macroRAFT agents, which contain DMAEMA moieties that require a low pH for the ionization, were compared to their quaternized counterparts, which possess permanent charges regardless of the pH of the medium.[47] Such property can be considered an advantage if we keep in mind that Laponite® is sensitive to pH and may undergo a gelation process or dissociate at low pH.[49, 50] The concentration of macroRAFT agent is another key parameter for the successful synthesis of nanocomposite materials with controlled morphologies through the REEP technique and was therefore carefully selected. The experiments carried out and the results obtained in terms of conversion X, $Z_{av.}$ and size dispersity are listed in Table 3.

Table 3. Emulsion copolymerization of MMA and BA (MMA:BA = 90:10 mol%) carried out with different macroRAFT agents (MR) at different concentrations, and results obtained in terms of monomer conversion, Z_{av} and size dispersity *(PdI)*.

Entry	**MR**	**[MR] (mM)**	**Clay (g L^{-1})**	**pH**	***X*** **(%)**	Z_{av} **(nm)**	***PdI***
R1*	-	0	5	10	24	293	0.25
R2	MR1q	2.28	5	10	75	-	-
$R2_{blank}$	MR1q	2.28	0	10	76	144	0.01
R3	MR2q	2.20	5	10	-	-	-
R4	MR2	2.20	5	6	67	71	0.12
R5	MR2	1.5	5	6	74	97	0.11
R6	MR2	1.1	5	6	72	135	0.14

*[AIBA] = 0.78 mM (for the other experiments the molar ratio macroRAFT agent:AIBA = 3:1).

For the experiment carried out in the absence of macroRAFT agent (R1), the system was unstable and a low conversion of 24% was achieved.

A concentration of 4.06 g L^{-1} (or 2.28 mM) was initially chosen for MR1q ($M_{n,\,theo}$ = 1780 g mol^{-1}) according to the adsorption isotherm of this copolymer[48] considering that, at this concentration, the surface of Laponite® is not only saturated with the copolymer, but there are some free chains in the aqueous phase to possibly stabilize the nanocomposite latex particles. For this experiment (R2), a final conversion of 75% was achieved after 6 hours of polymerization, however, the latex presented poor colloidal stability since the very early stages of the reaction. This polymerization was thus repeated under the same conditions but in the absence of Laponite® ($R2_{blank}$) and 76% conversion was achieved, with good colloidal stability (Z_{av} = 144 nm and *PdI* = 0.01). Indeed, it has been reported previously that short cationic polymer chains adsorb onto Laponite® in a flat extended configuration.[48] In this situation, it is very likely that the adsorbate will not be able to stabilize the nanocomposite latex particles. If the concentration of macroRAFT agents in the aqueous phase is insufficient to provide additional stability to these particles, aggregation may occur. In this aspect, the use of longer copolymer chains can be more interesting since they allow the formation of loops and tails along the chain, which are essential for stabilizing the hybrid latex particles. In

addition, a higher hydrophobicity of the macroRAFT agent helps to lower the electrostatic repulsion between cationic groups along the chain and increase the flexibility of the macromolecule, favoring the formation of long loops and tails. For these reasons, the macroRAFT agent P(DMAEMA$_{19}$-*co*-BA$_{14}$)-TTC (M_n = 4520 g L^{-1}, MR2 in Table 1) was designed as an alternative to overcome the stability issues caused by the use of P(DMAEMA$_{10}$-*co*-BA$_4$)-TTC. As the adsorption study of both quaternized molecules has shown,[48] the formation of loops and tails in the longer copolymer (MR2) also has an effect on the adsorption behavior, as it results in a higher adsorbed amount at saturation as compared to the shorter molecule (MR1).

For the synthesis of polymer/Laponite® hybrid latexes mediated by MR2, the use of the quaternized macromolecule resulted in the loss of the yellowish tone of the dispersion. Since a higher amount of methyl iodide was necessary for the quaternization of this copolymer compared to MR1, and the copolymer was not purified after quaternization, it is presumable that a degradation of the RAFT chain end C-S double bond could have been caused by residual methyl iodide under strong experimental conditions (sonication and heating). So, to avoid such degradation, unquaternized P(DMAEMA$_{19}$-*co*-BA$_{14}$)-TTC was used as an alternative, under a carefully selected pH. It is known that amidine groups of AIBA may suffer from hydrolysis at high pH values giving amide products that undergo thermolysis at a lower rate as compared to non hydrolyzed AIBA.[51] If pH is maintained below 7, the hydrolysis process can be minimized and radical formation can be assured. The polymerizations where AIBA was used as initiator were thus carried out at pH 6. In fact, at this pH value, the DMAEMA-based macroRAFT agent is protonated and, in addition, as seen by the pH scan carried out for the adsorption study,[48] this pH value is ideal for adsorption in DMAEMA-containing systems.

The macroRAFT agent concentration was selected based on the adsorption isotherm of this copolymer onto Laponite®,[48] which indicates that at a concentration of 0.7 mM of

macroRAFT agent, the clay surface is saturated and maximum adsorption has been reached. Beyond this point, the adsorption isotherm of MR2 reaches a clear plateau, unlike the quaternized counterpart, which is an indication of monolayer adsorption. It can be assumed that the formation of loops and tails is favored for the unquaternized macromolecule, whose conformation prevents the approach of additional macroRAFT agent. The presence of free macroRAFT agent in the aqueous phase, which is usually necessary for stabilization but cannot be excessive to avoid secondary nucleation, can thus be easily adjusted for MR2. For an initial concentration of 0.7 mM there should be not enough macroRAFT agent free in the aqueous phase to provide stability to the system. Therefore, three higher concentrations of P(DMAEMA$_{19}$-*co*-BA$_{14}$)-TTC were studied (R4 to R6, Table 3).

The use of MR2 at pH 6 resulted in the production of stable nanocomposite latexes, with conversions varying from 67 to 74% (Figure S2A, Supporting Information) regardless of its initial concentration. The higher macroRAFT agent concentration led to the lower particle size values (Table 3). However, the initial values of Z_{av} for all macroRAFT agent concentrations (Figure S2B, Supporting Information), showed that the use of a higher initial macroRAFT agent concentration (2.2 mM) led to the formation of macroRAFT agent/clay aggregates (Z_{av} ~150 nm). The strong interaction between this macroRAFT agent and Laponite® clay, *via* a monolayer adsorption, is well known.[48] It is therefore reasonable to assume that, if the concentration of free macroRAFT agent is high enough, a temporary aggregation phenomenon of macroRAFT agent/clay may occur prior to polymerization. The results show, however, that secondary nucleation might occur as polymerization starts, since a significant decrease in particle size is observed during polymerization.

Cryo-TEM images of latexes R1, R4, R5 and R6 are shown in Figure 1. Even though the latex synthesized in the absence of macroRAFT agent (R1) was unstable, indicating the formation of aggregated particles, non-spherical clay-containing latex particles of around 200 nm in diameter can be identified in Figure 1A. The non-spherical shape presented by these particles

can indicate that unstable primary particles suffered a fusion (or "aggregation") process leading to larger but individual final particles. The destabilization of the primary particles could be explained by an initial destabilization of clay platelets upon addition of the initiator (AIBA), which can adsorb on the clay surface through cation exchange and neutralize the surface charges of Laponite®. In addition, it is possible that the positively charged oligomers grown from or adsorbing on the clay surface during polymerization convert the clay from hydrophilic to hydrophobic and, as there is no surfactant in the system, at some point particle stabilization can no longer be ensured. Laponite® platelets can be seen either buried inside these large particles or located outside, at the particles surface. In the presence of 1.1 mM of macroRAFT agent (Figure 1B), stable dumbbell-like particles (one clay platelet sandwiched between two polymer nodes) were obtained. However, the final nanocomposite particles seem to have a tendency to merge, leading to rather large ($Z_{av.}$ = 135 nm) but stable particles with irregular contours. This could indicate that at the concentration of 1.1 mM of macroRAFT agent, the number of free molecules is not enough to generate individually stabilized particles. Indeed, similar but smaller (97 nm) particle morphology was obtained with 1.5 mM of macroRAFT agent (Figure 1C), and several Laponite® platelets can be seen almost fully covered with polymer, with only one of the extremities uncovered. When macroRAFT agent concentration was further increased to 2.2 mM (Figure 1D), most of the particles presented a dumbbell-like morphology, but more free latex particles (smaller than the hybrid ones) were obtained. The presence of a certain amount of free polymer particles, however, does not necessarily represent an issue for the final film and it can be easily minimized by increasing the inorganic concentration, if necessary.

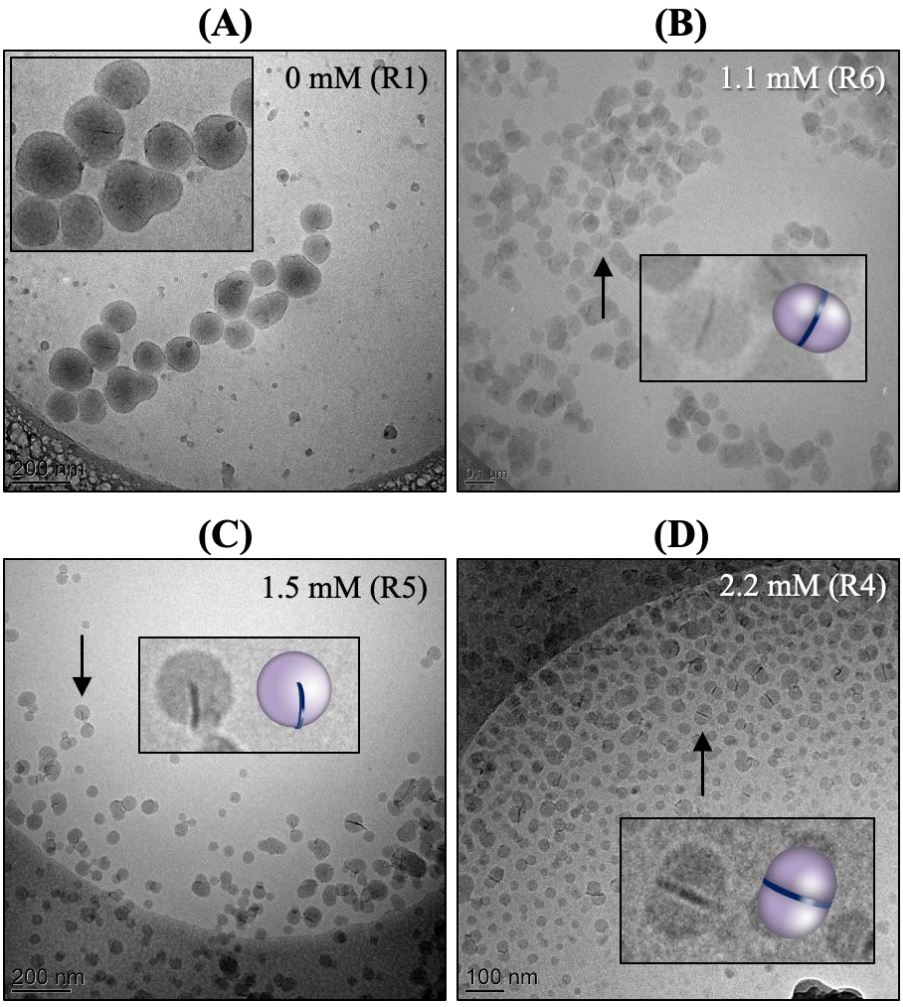

Figure 1. Cryo-TEM images of hybrid particles obtained by the copolymerization of MMA:BA 90:10 (mol:mol) in the presence of (A) 0 mM (R1), (B) 1.1 mM (R6), (C) 1.5 mM (R5) and (D) 2.2 mM (R4) of P(DMAEMA$_{19}$-*co*-BA$_{14}$)-TTC macroRAFT agent and 5 g L^{-1} of Laponite® at 80 °C. [AIBA] = 0.78 mM and pH = 10 for R1, while molar ratio macroRAFT agent:AIBA = 3:1 and pH = 6 for R4, R5 and R6.

In fact, the hybrid morphology obtained in the presence of a cationic macroRAFT agent is in line with what has been observed previously for non-ionic or anionic macroRAFT agents.[45] A few slight differences can be noticed though. In the case of the non-ionic or anionic macroRAFT agents, morphology control and stability are tightly dependent on the fraction of macroRAFT agent free in the continuous phase. If this fraction is excessively large, the polymerization locus shifts from the clay environment to the aqueous phase, and secondary nucleation is favored (resulting ultimately in stability loss). In the case of the cationic MR, thanks to their strong interaction with Laponite®, the polymerization locus can be effectively

driven to the basal surface of the clay and mostly encapsulated dumbbell particles with the platelets presenting little contact with water are obtained.

3.2. Toward film-forming latexes

To switch from a non-film-forming monomer composition to a suitable film-forming mixture, different monomer compositions were next tested. For this purpose, the macroRAFT agent chosen was MR2 and its concentration was fixed at 1.5 mM. In addition to the non-film-forming mixture MMA:BA 90:10 (R5, which is recalled in Table 4), two mixtures richer in BA and that are capable of forming films at room temperature were evaluated: MMA:BA 50:50 (R7) and Sty:BA 50:50 (R8). A more hydrophilic film-forming monomer mixture was tested as well, the MA:BA 80:20 (R9), as listed in Table 4.

Table 4. Emulsion polymerizations carried out with 1.5 mM of P(DMAEMA$_{19}$-*co*-BA$_{14}$)-TTC (MR2) and different monomer mixtures giving copolymers with different T_g values, and results obtained in terms of monomer conversion, Z_{av} and *PdI*.

Entry	**Monomer mixture m_1/m_2**	***Mixture* [mol/mol][a]**	**T_g [a] (°C)**	***X* (%)**	**Z_{av} (nm)**	***PdI***
R5	MMA/BA	90/10	72	74	97	0.11
R7	MMA/BA	50/50	−7	67	186	0.17
R8	Sty/BA	50/50	−7	72	-	-
R9	MA/BA	80/20	−7	48	306	0.39

[a] T_g of the copolymers calculated according to the Fox equation.

As shown in Figure S3, while 74% conversion was achieved for the MMA:BA 90:10 mixture (R5), the 50:50 MMA:BA and Sty:BA film-forming mixtures resulted in, respectively, conversions of 67 and 72%. A low conversion was obtained for the film-forming acrylate-based monomer mixture of R9 (MA:BA 80:20; X = 48%).

Figure 2 shows the cryo-TEM images of latexes R5 (A, which is recalled from Figure 1), R7 (B) and R8 (C). The images indicate that, for the film-forming mixtures MMA:BA 50:50 (R7)

and Sty:BA 50:50 (R8), similar results were obtained in terms of particle morphology, with the formation of a majority of large armored particles. The effect of monomer composition seems to agree with what has been reported in the literature.[47] When the T_g of the polymeric shell is low, inorganics tend to migrate to the polymer/water interface during polymerization, the system searching for a thermodynamically favored morphology.

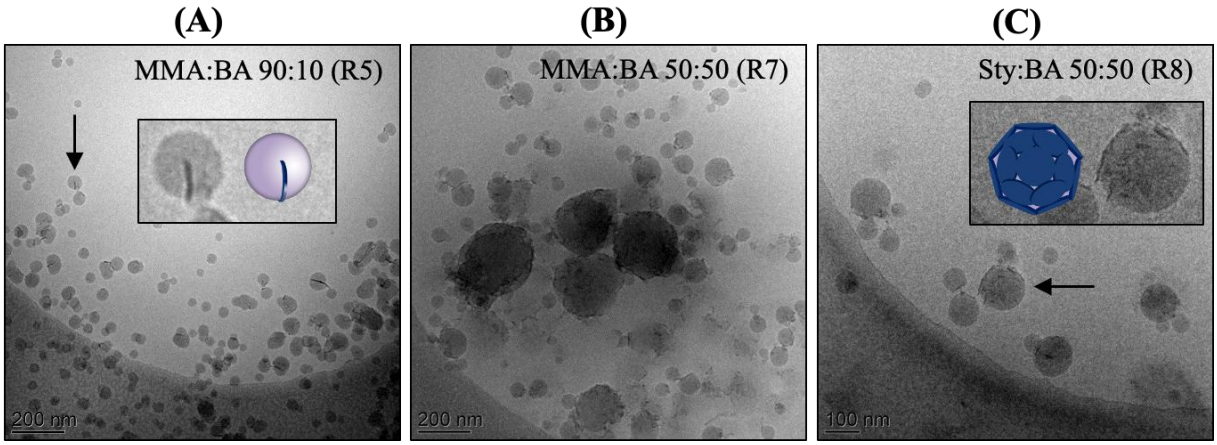

Figure 2. Cryo-TEM images of hybrid particles obtained by the copolymerization of (A) MMA:BA 90:10 (R5), (B) MMA:BA 50:50 (R7) and (C) Sty:BA 50:50 (R8) (molar ratios) in the presence of 1.5 mM of P(DMAEMA$_{19}$-*co*-BA$_{14}$)-TTC macroRAFT agent and 5 g L^{-1} of Laponite® at 80 °C and pH 6.

A blank experiment was carried out to verify the particle size evolution in the film-forming formulation MMA:BA 50:50 in the absence of clay (R7$_{blank}$, shown in Figure S4). A comparison between both experiments indicates similar results in terms of overall and instantaneous conversions. The polymerization carried out in the absence of clay, however, presented a different profile of particle size evolution, with large particle sizes obtained only in the presence of clay, which suggests a different nucleation mechanism and indicate that the soft character of the copolymers is not responsible for the poor stability of the initial hybrid particles. The formation of larger particles for experiments carried out with the film-forming monomer composition in the presence of clay platelets could be, essentially, a matter of polymer/water interfacial tensions. As macroRAFT agent partitioning should be independent of the monomer composition and the polymer/water interfacial tension is higher for the more hydrophobic P(MMA-*co*-BA) (50/50, R7) or P(Sty-*co*-BA) (50:50, R8) latexes than for the

more hydrophilic P(MMA-*co*-BA) (90:10, R5) particles, intuitively, one should consider that more (free) macroRAFT agent is needed to stabilize R7 and R8 than R5. The amount of free macroRAFT agent could be insufficient in the case of a less polar interface to maintain stability, resulting in the formation of larger particles with an armored morphology – the clay platelets locating themselves at the polymer/water interface to minimize contact with the hydrophobic polymer, which is also facilitated by the low T_g.

Nonetheless, to confirm this hypothesis, it is fundamental to evaluate the copolymerization of the more hydrophilic film-forming mixture of MA and BA. The lower conversion obtained in this copolymerization (R9, X = 48%) can be attributed to monomer evaporation, which may happen through the condenser and is more critical in the film-forming monomer mixture composed of MA, since this monomer has a lower boiling point (80 °C) than MMA (101 °C). As the initiator ADIBA has higher decomposition rate constant and a half-life decomposition time in water, at 80 °C, nearly 3 times lower than AIBA,[52] it was used to replace AIBA in the emulsion polymerizations, giving the possibility to reduce the reaction temperature. So, the emulsion polymerization carried out with the MA:BA film-forming monomer mixture, which presented an unsatisfactory conversion, was repeated with ADIBA instead of AIBA, at 60 ºC (R10, Figure 3). The final conversion was increased to 72%, which confirms the above-mentioned assumptions. In addition, the latex R10 was stable, and mostly composed of dumbbell-like and few Janus particles with a final particle size of 110 nm (Figure 4B), which supports the relationship between the formation of larger particles and the more hydrophobic nature of MMA:BA 50:50 monomer composition.

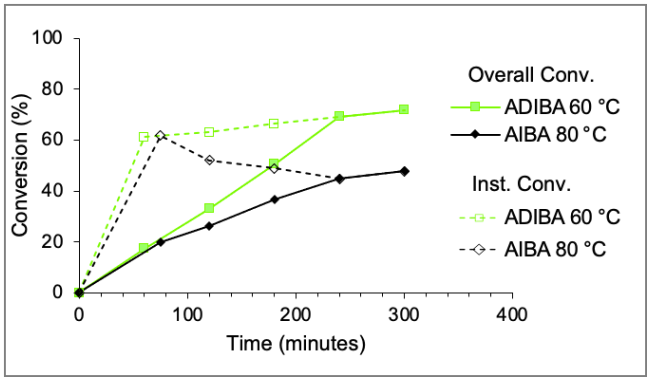

Figure 3. Overall monomer conversion (straight line) and instantaneous conversion (dashed line) versus time for the polymerization of MA:BA 80:20 (molar ratio) in the presence of 1.5 mM of P(DMAEMA$_{19}$-*co*-BA$_{14}$)-TTC macroRAFT agent, 5 g L^{-1} of Laponite® and different initiators: AIBA at 80 °C (R9) and ADIBA at 60 °C (R10).

3.3. Effect of clay content

To study the effect of the clay content in the polymerization and in the formation of the hybrid particles, three different systems were compared to the formulation of R10, containing 5 g L^{-1} of Laponite® (which also represents 5% weight of clay, based on the monomer mass), 1.5 mM of macroRAFT agent and using the film-forming formulation with MA and BA. A blank experiment was carried out in the absence of clay (R10$_{blank}$) and two experiments were carried out increasing the Laponite® content to 10 g L^{-1}, with two different macroRAFT agent concentrations: 1.5 (R11) and 3 mM (R12). All polymerizations were initiated by ADIBA, and results are shown in Table 5, while the evolution of overall and instantaneous conversions is shown in Figure S5.

Table 5. Conditions used in the synthesis of hybrid latexes by RAFT-mediated emulsion polymerization of MA:BA (80:20 mol%) in the presence of P(DMAEMA$_{19}$-*co*-BA$_{14}$)-TTC macroRAFT agent at pH 6 and results obtained in terms of monomer conversion, Z_{av} and size *PdI*.

Entry	**Clay (g L^{-1})**	**[MR] (mM)**	***X*** **(%)**	**Z_{av} (nm)**	***PdI***
R10	5	1.5	72	110	0.25
R10$_{blank}$	0	1.5	86	25	0.17
R11	10	1.5	65	300	0.40
R12	10	3	72	75	0.13
R12$_{blank}$	0	3	79	22	0.12

Cryo-TEM images of the latexes are shown in Figure 4. A comparison between images (A), (B) and (C), which correspond respectively to 0, 5 and 10 g L^{-1} of Laponite®, for a fixed macroRAFT agent concentration of 1.5 mM, reveals that the variation in the clay content results in a change in the particles size. While very small particles (Z_{av} = 25 nm) were obtained in the absence of clay, hybrid particles with dumbbell and Janus morphologies of around 110 nm (from DLS) were formed in the presence of 5 g L^{-1} of Laponite®, which again indicates that the platelets play a crucial role in the mechanism of particle formation. Furthermore, if the clay content is increased to 10 g L^{-1}, 1.5 mM of macroRAFT agent is no longer enough to provide stability to the growing particles and they aggregate forming armored structures. A higher concentration of macroRAFT agent (3 mM) was used to guarantee the stabilization of particles in the presence of 10 g L^{-1} of Laponite®, as shown in Figure 3D. In this case, smaller dumbbell particles were formed (~75 nm), suggesting that the particle morphology is controlled by the amount of free macroRAFT agent.

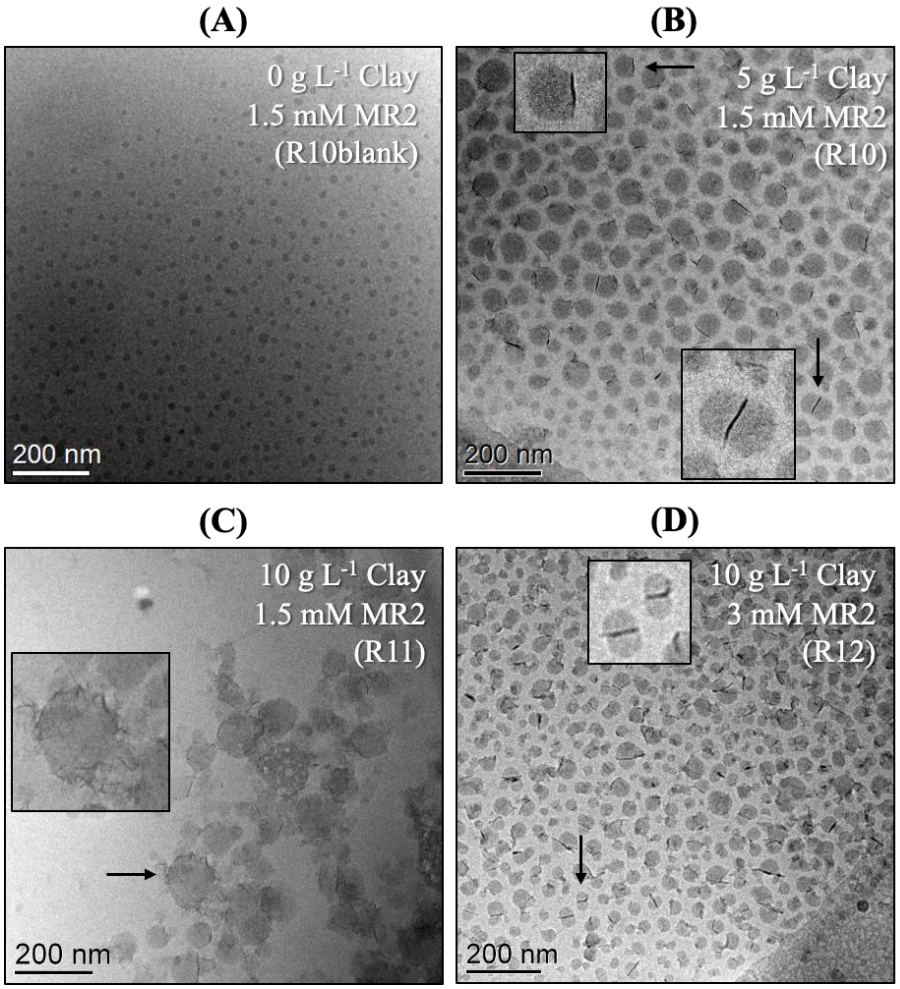

Figure 4. Cryo-TEM images of hybrid particles obtained by the copolymerization of MA:BA 80:20 (molar ratio) using ADIBA as initiator at 60 °C in the presence of (A) 1.5 mM of P(DMAEMA$_{19}$-*co*-BA$_{14}$)-TTC macroRAFT agent and 0% Laponite® (R10$_{blank}$); (B) 1.5 mM of macroRAFT agent and 5 g L^{-1} of Laponite® (R10); (C) 1.5 mM of macroRAFT agent and 10 g L^{-1} of Laponite® (R11) and (D) 3 mM of macroRAFT agent and 10 g L^{-1} of Laponite® (R12).

3.4. Mechanical behavior

The P(MA-*co*-BA) nanocomposite latexes with different Laponite® contents, R10 and R12, with hybrid particles of predominant dumbbell morphology, were selected for the production of films. Films were also formed from the clay-free counterparts (denominated matrix), obtained by copolymerization of MA with BA under the same conditions as R10 and R12 but in the absence of clay. All films were obtained by the casting method, their thermo-mechanical behavior was determined by DMA, and their microstructure was investigated by FIB-SEM observation of 2D cross-sections of the material, as shown in Figure 5.

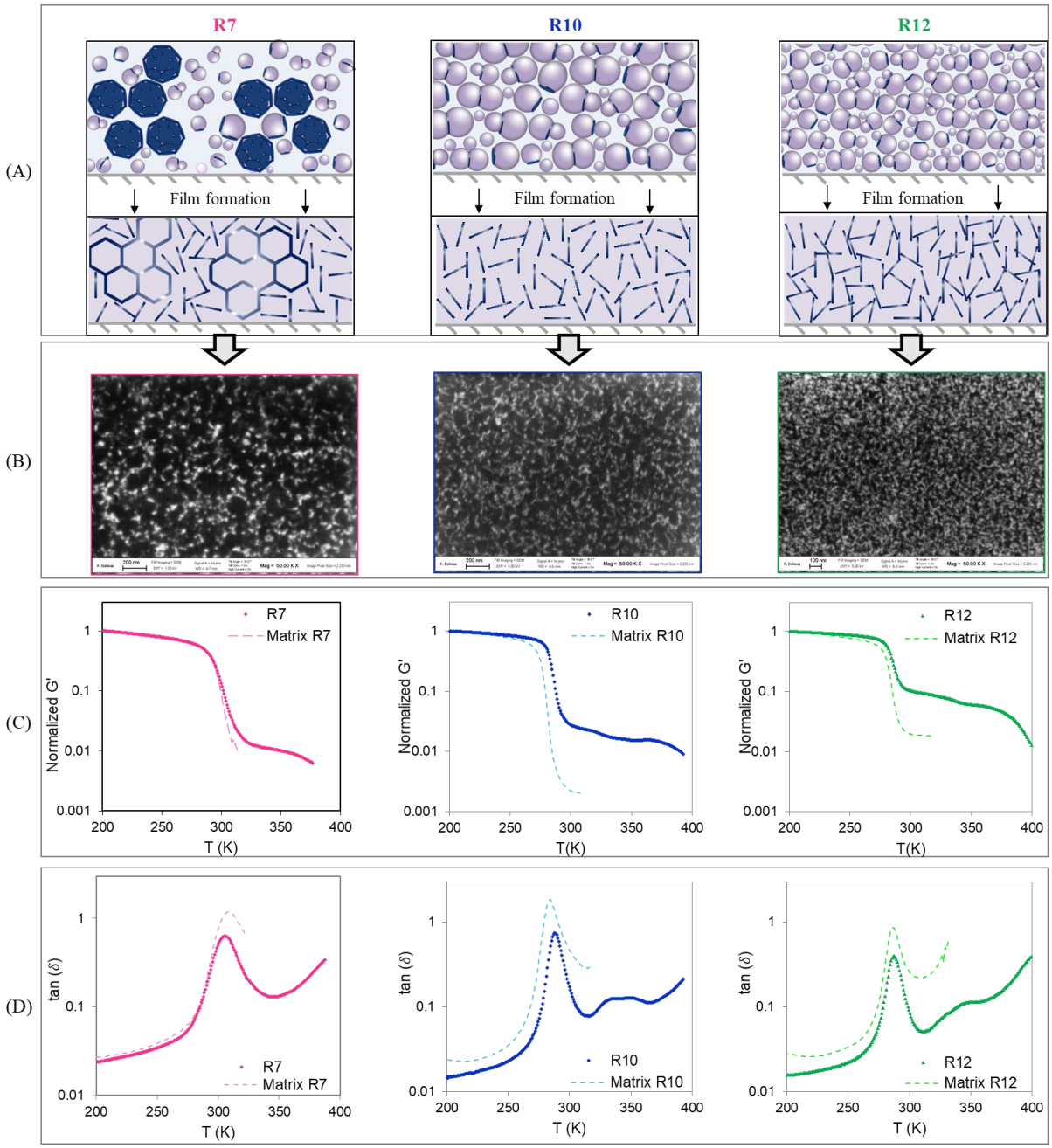

Figure 5. (A) Schematic representation of the expected homogeneous and structured organization of the composite particles obtained after the film-formation process; (B) FIB–SEM observation, (C) Storage shear modulus, G′, as a function of temperature and (D) Loss Factor, tan(δ), as a function of temperature for the Laponite® nanocomposite films and for the corresponding unfilled matrices of R7 (MMA:BA 50:50 mol%, 5 wt% of clay and 1.5 mM of MR2), R10 (MA:BA 80:20 mol%, 5 wt% of clay and 1.5 mM of MR2); and R12 (MA:BA 80:20 mol%, 10 wt% of clay and 3 mM of MR2). The storage moduli have been normalized at 1 GPa at 200 K for all samples.

Besides the different clay contents, these latex samples also differ in the concentration of P(DMAEMA$_{19}$-*co*-BA$_{14}$)-TTC macroRAFT agent. As schematically represented in Figure 5A, after film forming, the dumbbell morphologies are expected to lead to nanostructured

composite films with a homogeneous distribution of the platelets in the polymer matrix that are likely to present interesting mechanical behaviors. For purposes of comparison, the latex obtained in R7 (MMA:BA 50:50 mol%) containing both dumbbell and clay-armored particles was also selected for this study in order to shed light on the effect of particle morphology.

To better understand the effect exerted by Laponite® on the final mechanical properties of the films, the resulting nanocomposite films had their microstructure investigated by imaging a 2D cross-section of the material via FIB–SEM. Images are shown in Figure 5B. The different contrasts in the images indicate the presence of Laponite® platelets (which are the bright phase) and the polymer matrix (which is the dark background). However, the small size of Laponite® particles does not allow an individual observation of platelets. It is possible to see, nonetheless, that there is a homogeneous distribution of the platelets in the polymer matrix, generating, at large scale, a network structure. These connected structures are even more pronounced for the higher clay content.

The mechanical behavior of the Laponite®-reinforced films, as well as of the corresponding pure polymer matrices, was investigated by DMA and the plotting of the shear storage modulus G′ versus the temperature is shown in Figure 5C. Due to the large uncertainty on the thickness of such thin film samples (which leads to a three times higher uncertainty on the modulus value), the modulus curves of all samples have been normalized at 1 GPa at 200 K. The expected modulus for the unfilled matrix should, in fact, be around this value, but the filled samples would be expected to have a modulus between 2 to 3 times higher. This error, however, has no consequences on the following discussion, which is based on the modulus value at temperature above that of the main relaxation, since the mechanical contrast between the inorganic particles and the matrix is then expected to be of the order of a decade or more. [52] As shown in Figure 5C, the storage moduli, G′, of the nanocomposites are characterized by a two-step flowing profile. A first drop of the modulus can be observed at low temperatures, followed by a long plateau and a second drop of the modulus at high temperatures. The first

drop, observed for matrices as well as for nanocomposites, is related to the alpha relaxation of the matrix. As shown in Table 4, the T_g of the hydrophobic part of the self-assembled copolymers formed (−7 °C, according with Fox equation) is in agreement with the temperature at which this drop occurs.

It is worth mentioning that the matrices alone present a modulus value in the rubbery state quite high even without filler, which is remarkable. It can be noticed that the increase in the weigh fraction of macroRAFT agent within the matrix R12 (14 wt%), as compared to matrix R10 (6.7 wt%), led to an increase in the modulus in the rubbery plateau, by a factor 10. Such observation indicates that, despite the absence of clay platelets, a rigid phase is present in these systems. Indeed, a mechanical reinforcement effect has already been reported for a similar self-assembled system with a PAA-based macroRAFT agent and attributed to intermolecular ionic interactions between the carboxylate groups of AA and the counter-ions present in the system. In terms of microstructure, as proposed by Chenal et al.[54] and Dalmas et al.[46] and schematically represented in Figure 6, core-shell-based films are formed by a soft polymer core and macroRAFT shell that behaves as the hard phase, in the formation of a thin honeycomb percolating network. In the case of the present work, it is hypothesized that the self-assembly of hydrophobic/hydrophilic block copolymers form soft hydrophobic P(MA-BA) spheres (core) that are connected to each other by rigid hydrophilic links through intermolecular ionic interactions between the amine groups of DMAEMA and the counter-ions introduced for their protonation, creating a hard and percolating phase in the matrix that is responsible for the stiffening of the material.

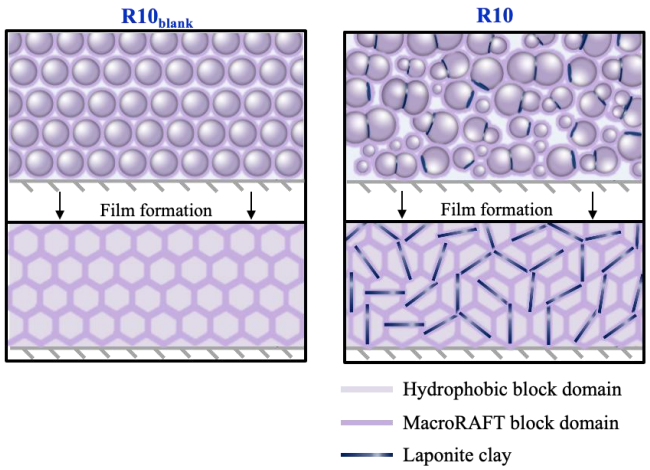

Figure 6. Hypothetical schematic representation of the hard percolating phase formed by the macroRAFT agent in the matrix and in the nanocomposite after the film-formation process.

A comparison of the storage modulus, G′, between the matrix and the corresponding nanocomposite in the rubbery plateau shows that there is an additional stiffening effect due to the presence of the platelets. An increase in modulus of around 10 times the one of the matrix is observed with the addition of 5 wt% of Laponite® (Figure 5C-R10). A stronger reinforcement seems to be obtained in this case than for similar systems reported previously with pure macroRAFT and Fe(III)acetylacetonate (6 MPa)[55] or LDH (10-20 MPa).[46] Although less important, a similar reinforcing effect is observed in the mechanical properties of the material when the nanocomposite is filled with 10 wt% of Laponite® (Figure 5C-R12). Such high enhancements in the presence of clay platelets can be attributed to the formation of stiff networks within the materials and can be described by the mechanical percolation model,[55] which considers that there is a parallel mechanical coupling of the rigid phase (the network of platelets) with the soft phase (the polymer matrix). Two percolating networks are therefore expected: one formed by the direct contact between Laponite® platelets and a second one formed by the macroRAFT chains. As a consequence, stress can be transferred from one platelet to another either through their direct contact, or through the rigid part of the matrix in between them. This mixed network of clay and hydrophilic polymer, which is stiffer than the

matrix, has already been reported for graphene[53] and LDH[56] nanocomposites. In the case of Laponite, the arrangement of the platelets into a stiff percolating network can be tentatively attributed to the dumbbell and Janus morphology of the particles. Indeed, even though the steric hindrance of the spheres in dumbbell morphology can be unfavorable for the approach between the clays, in an encapsulated-like behavior, the presence of Janus particles can potentially favor platelet-platelet interactions within the polymer matrix allowing clay-clay contact to take place through the uncoated edges of the dumbbell and Janus structures.

In Figure 5D, which shows the Loss Factor tan(δ) as a function of temperature, the main relaxation temperature (Tα), attributed to the polymer phase, as well as the second relaxation peak, in the case of R10 and R12, can be observed. Finally, at high enough temperatures, the polymer begins to flow, as evidenced by a decrease in modulus. As already mentioned before, the DMAEMA-based macroRAFT agent adsorbs on the clay platelets by ionic bonds. Although strong in the beginning, it is possible that the interaction between the clay and macroRAFT agents becomes weak at high temperatures, allowing an increase in the mobility of the clays and, consequently, a rapid decrease in modulus with the temperature.

Interestingly, a minor effect of the armored morphology of R7 on modulus can be observed (Figure 5C-R7), unlike the purely dumbbell morphology of R10 and R12. However, highly percolating nanocomposite films resulting from armored layered structures are known to show high rubber modulus plateau, as already reported previously for LDH hybrid films,[46] for example. But the heterogeneity of sample R7 in terms of particle morphology, with the presence of small dumbbell-like and larger clay-armored particles, might have been detrimental to the mechanical properties of the film. In this system, percolation was not promoted as in typical purely armored or purely dumbbell systems. Instead of getting the most of both morphologies, having a mixture of them may have resulted in the disturbance of the percolating path.

4. Conclusions

The preparation of polymer/Laponite® nanocomposite latexes by cationic macroRAFT agent-mediated emulsion polymerization via the REEP strategy is described. The molar mass of these copolymers played a crucial role in the stabilization of the nanocomposite latex particles as short copolymers were unable to efficiently stabilize the particles while the longer chains were more efficient in this respect. The strong adsorption of the DMAEMA-based copolymer and good wettability of the inorganic surface with macroRAFT agent led to the formation of partially encapsulated particles, with clay platelets sandwiched between two polymer particles and, in some cases, with the edges and the basal surfaces covered with polymer, when a non-film-forming composition (MMA:BA 90:10) was used.

For film-forming monomer mixtures, the more hydrophobic character of the mixture (MMA:BA and Sty:BA 50:50) led to the formation of armored particles. In the presence of 5 g L^{-1} of clay, the use of a more hydrophilic film-forming monomer mixture (MA:BA 80:20) resulted in dumbbell morphologies with particle size of ~100 nm. On the other hand, increasing the clay content to 10 g L^{-1} for a fixed macroRAFT agent concentration resulted in the formation of armored structures, indicating that, to guarantee the stability of the dumbbell particles, it is crucial to increase the macroRAFT agent concentration as well.

FIB-SEM images of the more hydrophilic film-forming formulations with different clay contents indicated a homogeneous distribution of the platelets within the polymer matrix. In terms of mechanical properties, the presence of the clay platelets, as well as of the macroRAFT agents, increased the stiffness of the material in comparison to the pure polymer matrix. Such enhancement could be attributed to the formation of a connected network of platelets in the matrix, as well as a percolating network formed by the DMAEMA-based macroRAFT chains. In this aspect, the dumbbell morphology of the particles might have been crucial for the arrangement of the platelets in this mechanical percolation structure.

For a successful encapsulation process, the existence of a strong interaction between the macroRAFT agent and the surface of the clay seems to be a crucial factor, since it defines the clay environment as the polymerization locus. Even though DMAEMA-based macroRAFT agents present a strong adsorption onto Laponite®, the different charges of the edges and the surface of the platelets led to the production of mostly bare-edged particles, such as in the dumbbell morphology. In fact, the lamellar shape of the platelets, their high aspect ratio and surface energy, added to the opposite charges on the surface and on the edges of the platelets, make the complete and individual encapsulation of the platelets with a thin polymer layer that maintains the shape anisotropy of the particles difficult to be achieved. In this aspect, another approach to efficiently cover the edges of the clay platelets has been investigated in our group and will be reported in a subsequent paper.

Supporting Information

Detailed equations for calculation of instantaneous and overall conversions. Evolution of overall monomer conversion and instantaneous conversion with time and average hydrodynamic diameters and size dispersity with conversion during the RAFT-mediated emulsion polymerizations.

Acknowledgements: The authors gratefully acknowledge financial support from the funding agencies FAPESP (2010/19919-6), CNRS and FCT/MEC from Brazil, France and Portugal, respectively, and IUPAC for enabling the ENCIRCLE (Polymer encapsulation of anisotropic inorganic particles by RAFT-mediated emulsion polymerization) project, Baptiste Gary from MATEIS Laboratory (INSA of Lyon) for DMA and FIB-SEM analysis and Pierre-Yves Dugas (CP2M) for cryo-TEM images.

Keywords: Laponite®, surfactant-free emulsion polymerization, RAFT, encapsulation, nanocomposites

References

1. Kotal, M.; Bhowmick, A. K., Polymer nanocomposites from modified clays: Recent advances and challenges. *Prog. Polym. Sci.* **2015,** *51*, 127-187.
2. Bhattacharya, M., Polymer Nanocomposites—A Comparison between Carbon Nanotubes, Graphene, and Clay as Nanofillers. *Materials* **2016,** *9*, 262-297.
3. Wypych, F.; Bergaya, F.; Schoonheydt, R. A., From polymers to clay polymer nanocomposites. In *Developments in Clay Science*, Schoonheydt, R.; Johnston, C. T.; Bergaya, F., Eds. Elsevier: 2018; Vol. 9, pp 331-359.
4. Prevot, V.; Bourgeat-Lami, E., Recent advances in layered double hydroxide/polymer latex nanocomposites: from assembly to in situ formation. In *Layered Double Hydroxide Polymer Nanocomposites*, Thomas, S.; Daniel, S., Eds. Woodhead Publishing: 2020; pp 461-495.
5. Kiliaris, P.; Papaspyrides, C. D., Polymer/layered silicate (clay) nanocomposites: An overview of flame retardancy. *Prog. Polym. Sci.* **2010,** *35*, 902-958.
6. Tan, B.; Thomas, N. L., A review of the water barrier properties of polymer/clay and polymer/graphene nanocomposites. *J. Membr. Sci.* **2016,** *514*, 595-612.
7. Zhu, T. T.; Zhou, C. H.; Kabwe, F. B.; Wu, Q. Q.; Li, C. S.; Zhang, J. R., Exfoliation of montmorillonite and related properties of clay/polymer nanocomposites. *Appl. Clay Sci.* **2019,** *169*, 48-66.
8. Yano, K.; Usuki, A.; Okada, A.; Kurauchi, T.; Kamigaito, O., Synthesis and properties of polyimide–clay hybrid. *J. Polym. Sci. Part A: Polym. Chem.* **1993,** *31*, 2493-2498.
9. Bourgeat-Lami, E., Organic-Inorganic Nanostructured Colloids. *J. Nanosci. Nanotechnol.* **2002,** *2*, 1-24.
10. Balmer, J. A.; Schmid, A.; Armes, S. P., Colloidal nanocomposite particles: quo vadis? *J. Mater. Chem.* **2008,** *18*, 5722-5730.
11. Thickett, S. C.; Teo, G. H., Recent advances in colloidal nanocomposite design via heterogeneous polymerization techniques. *Polym. Chem.* **2019,** *10*, 2906-2924.
12. Mittal, V., Polymer Nanocomposites in Emulsion and Suspension: an Overview. In *Polymer Nanocomposites by Emulsion and Suspension Polymerization*, The Royal Society of Chemistry: 2011; pp 1-31.
13. Bourgeat-Lami, E.; Sheibat-Othman, N.; Dos Santos, A. M., Polymer–Clay Nanocomposite Particles and Soap-free Latexes Stabilized by Clay Platelets: State of the Art and Recent Advances. In *Polymer Nanocomposites by Emulsion and Suspension Polymerization*, The Royal Society of Chemistry: 2011; pp 269-311.
14. Faucheu, J.; Gauthier, C.; Chazeau, L.; Cavaillé, J.-Y.; Mellon, V.; Lami, E. B., Miniemulsion polymerization for synthesis of structured clay/polymer nanocomposites: Short review and recent advances. *Polymer* **2010,** *51*, 6-17.
15. Wang, T.; Keddie, J. L., Design and fabrication of colloidal polymer nanocomposites. *Adv. Colloid Interface Sci.* **2009,** *147-148*, 319-332.
16. Bourgeat-Lami, E.; Lansalot, M., Organic/inorganic composite latexes: the marriage of emulsion polymerization and inorganic chemistry. *Adv. Polym. Sci.* **2010,** *233*, 53-123.

17. Gharieh, A.; Khoee, S.; Mahdavian, A. R., Emulsion and miniemulsion techniques in preparation of polymer nanoparticles with versatile characteristics. *Adv. Colloid Interface Sci.* **2019,** *269*, 152-186.
18. Negrete-Herrera, N.; Putaux, J.-L.; David, L.; De Haas, F.; Bourgeat-Lami, E., Polymer/Laponite composite latexes: Particle morphology, film microstructure, and properties. *Macromol. Rapid Commun.* **2007,** *28*, 1567-1573.
19. Bourgeat-Lami, E.; Guimarães, T. R.; Pereira, A. M. C.; Alves, G. M.; Moreira, J. C.; Putaux, J.-L.; dos Santos, A. M., High Solids Content, Soap-Free, Film-Forming Latexes Stabilized by Laponite Clay Platelets. *Macromol. Rapid Commun.* **2010,** *31*, 1874-1880.
20. Delafresnaye, L.; Dugas, P.-Y.; Dufils, P.-E.; Chaduc, I.; Vinas, J.; Lansalot, M.; Bourgeat-Lami, E., Synthesis of clay-armored poly(vinylidene chloride-co-methyl acrylate) latexes by Pickering emulsion polymerization and their film-forming properties. *Polym. Chem.* **2017,** *8*, 6217-6232.
21. Dastjerdi, Z.; Cranston, E. D.; Berry, R.; Fraschini, C.; Dubé, M. A., Polymer Nanocomposites for Emulsion-Based Coatings and Adhesives. *Macromol. React. Eng.* **2019,** *13*, 1800050.
22. Kausar, A., Emulsion polymer derived nanocomposite: a review on design and tailored attributes. *Polym. Plast. Tech. Mat.* **2020,** *59*, 1737-1750.
23. Zetterlund, P. B.; Thickett, S. C.; Perrier, S.; Bourgeat-Lami, E.; Lansalot, M., Controlled/Living Radical Polymerization in Dispersed Systems: An Update. *Chem. Rev.* **2015,** *115*, 9745−9800.
24. Bourgeat-Lami, E.; D'Agosto, F.; Lansalot, M., Synthesis of Nanocapsules and Polymer/Inorganic Nanoparticles Through Controlled Radical Polymerization At and Near Interfaces in Heterogeneous Media. *Adv. Polym. Sci.* **2016**, *270*,123-161.
25. Cenacchi-Pereira, A.; Grant, E.; D'Agosto, F.; Lansalot, M.; Bourgeat-Lami, E., Encapsulation with the Use of Controlled Radical Polymerization. In *Encyclopedia of Polymeric Nanomaterials*, Kobayashi, S.; Müllen, K., Eds. Springer Berlin Heidelberg: Berlin, Heidelberg, 2014; pp 1-13.
26. Nguyen, D.; Zondanos, H. S.; Farrugia, J. M.; Serelis, A. K.; Such, C. H.; Hawkett, B. S., Pigment Encapsulation by Emulsion Polymerization Using Macro-RAFT Copolymers. *Langmuir* **2008,** *24*, 2140-2150.
27. Daigle, J.-C., General method for the preparation of inorganic-organic core shell nanoparticles. *PMSE Preprints* **2008,** *98*, 685.
28. Das, P.; Zhong, W.; Claverie, J. P., Copolymer nanosphere encapsulated CdS quantum dots prepared by RAFT copolymerization: synthesis, characterization and mechanism of formation. *Colloid Polym. Sci.* **2011,** *289*, 1519-1533.
29. Das, P.; Claverie, J. P., Synthesis of single‐core and multiple‐core core‐shell nanoparticles by RAFT emulsion polymerization: Lead sulfide‐copolymer nanocomposites. *J. Polym. Sci. Part A: Polym. Chem.* **2012,** *50*, 2802-2808.
30. Zgheib, N.; Putaux, J.-L.; Thill, A.; Bourgeat-Lami, E.; D'Agosto, F.; Lansalot, M., Cerium oxide encapsulation by emulsion polymerization using hydrophilic macroRAFT agents. *Polym. Chem.* **2013,** *4*, 607-614.
31. Li, K.; Dugas, P.-Y.; Bourgeat-Lami, E.; Lansalot, M., Polymer-encapsulated γ-Fe2O3 nanoparticles prepared via RAFT-mediated emulsion polymerization. *Polymer* **2016,** *106*, 249-260.
32. Nguyen, D.; Pham, B. T. T.; Huynh, V.; Kim, B. J.; Pham, N. T. H.; Bickley, S. A.; Jones, S. K.; Serelis, A.; Davey, T.; Such, C.; Hawkett, B. S., Monodispersed polymer encapsulated superparamagnetic iron oxide nanoparticles for cell labeling. *Polymer* **2016,** *106*, 238-248.

33. Bourgeat-Lami, E.; França, A. J. P. G.; Chaparro, T. C.; Silva, R. D.; Dugas, P. Y.; Alves, G. M.; Santos, A. M., Synthesis of Polymer/Silica Hybrid Latexes by Surfactant-Free RAFT-Mediated Emulsion Polymerization. *Macromolecules* **2016,** *49*, 4431-4440.
34. van Herk, A. M., Polymer Encapsulation of Single Clay Platelets by Emulsion Polymerization Approaches, Thermodynamic, and Kinetic Factors. *Macromol. React. Eng.* **2015,** *10*, 22-28.
35. Ali, S. I.; Heuts, J. P. A.; Hawkett, B. S.; van Herk, A. M., Polymer encapsulated gibbsite nanoparticles: efficient preparation of anisotropic composite latex particles by RAFT-based starved feed emulsion polymerization. *Langmuir* **2009,** *25*, 10523-10533.
36. Zhong, W.; Zeuna, J. N.; Claverie, J. P., A versatile encapsulation method of noncovalently modified carbon nanotubes by RAFT polymerization. *J. Polym. Sci. Part A: Polym. Chem.* **2012,** *50*, 4403-4407.
37. Nguyen, D.; Such, C. H.; Hawkett, B. S., Polymer coating of carboxylic acid functionalized multiwalled carbon nanotubes via reversible addition-fragmentation chain transfer mediated emulsion polymerization. *J. Polym. Sci. Part A: Polym. Chem.* **2013,** *51*, 250-257.
38. Huynh, V. T.; Nguyen, D.; Such, C. H.; Hawkett, B. S., Polymer Coating of Graphene Oxide via Reversible Addition-Fragmentation Chain Transfer Mediated Emulsion Polymerization. *J. Polym. Sci. Part A: Polym. Chem.* **2015,** *53*, 1413-1421.
39. Perreira, A. C.; Pearson, S.; Kostadinova, D.; Leroux, F.; D'Agosto, F.; Lansalot, M.; Bourgeat-Lami, E.; Prévot, V., Nanocomposite latexes containing layered double hydroxides via RAFT-assisted encapsulating emulsion polymerization. *Polym. Chem.* **2017,** *8*, 1233-1243.
40. Pearson, S.; Pavlovic, M.; Augé, T.; Torregrossa, V.; Szilagyi, I.; D'Agosto, F.; Lansalot, M.; Bourgeat-Lami, E.; Prévot, V., Controlling the Morphology of Film-Forming, Nanocomposite Latexes Containing Layered Double Hydroxide by RAFT-Mediated Emulsion Polymerization. *Macromolecules* **2018,** *51*, 3953-3966.
41. Mballa Mballa, M. A.; Ali, S. I.; Heuts, J. P. A.; van Herk, A. M., Control of the anisotropic morphology of latex nanocomposites containing single montmorillonite clay particles prepared by conventional and reversible addition‐fragmentation chain transfer based emulsion polymerization. *Polym. Int.* **2012,** *61*, 861-865.
42. Guimaraes, T. R.; Chaparro, T. d. C.; D'Agosto, F.; Lansalot, M.; dos Santos, A. M.; Bourgeat-Lami, E., Synthesis of multi-hollow clay-armored latexes by surfactant-free emulsion polymerization of styrene mediated by poly(ethylene oxide)-based macroRAFT/Laponite complexes. *Polym. Chem.* **2014,** *5*, 6611-6622.
43. Silva, R. D.; Stefanichen Monteiro, I.; Chaparro, T. d. C.; Silva Hardt, R.; Giudici, R.; Barros-Timmons, A.; Bourgeat-Lami, E.; Martins dos Santos, A., Investigation of the Adsorption of Amphipathic macroRAFT Agents onto Montmorillonite Clay. *Langmuir* **2017,** *33*, 9598-9608.
44. Silva, R. D.; Chaparro, T. d. C.; Monteiro, I. S.; Dugas, P.-Y.; D'Agosto, F.; Lansalot, M.; Martins dos Santos, A.; 'Bourgeat-Lami, E., Tailoring the Morphology of Polymer/Montmorillonite Hybrid Latexes by Surfactant-Free Emulsion Polymerization Mediated by Amphipathic MacroRAFT Agents. *Macromolecules* **2019,** *52*, 4979-4988.
45. Chaparro, T. C.; Silva, R. D.; Dugas, P.-Y.; D'Agosto, F.; Lansalot, M.; Martins dos Santos, A.; Bourgeat-Lami, E., Laponite®-based colloidal nanocomposites prepared by RAFT-mediated surfactant-free emulsion polymerization: the role of non-ionic and anionic macroRAFT polymers in stability and morphology control. *Polym. Chem.* **2021,** *12*, 69-81.
46. Dalmas, F.; Pearson, S.; Gary, B.; Chenal, J.-M.; Bourgeat-Lami, E.; Prévot, V.; Chazeau, L., Tailored microstructure and mechanical properties of nanocomposite films made from polyacrylic/LDH hybrid latexes synthesized by RAFT-mediated emulsion polymerization. *Polym. Chem.* **2018,** *9*, 2590-2600.

47. Mballa Mballa, M. A.; Ali, S. I.; Heuts, J. P. A.; van Herk, A. M., Control of the anisotropic morphology of latex nanocomposites containing single montmorillonite clay particles prepared by conventional and reversible addition‐fragmentation chain transfer based emulsion polymerization. *Polym. Int.* **2012,** *61*, 861-865.
48. Chaparro, T. d. C.; Silva, R. D.; Monteiro, I. S.; Barros-Timmons, A.; Giudici, R.; Martins dos Santos, A.; Bourgeat-Lami, E., Interaction of Cationic, Anionic, and Nonionic Macroraft Homo- and Copolymers with Laponite Clay. *Langmuir* **2019,** *35*, 11512-11523.
49. Cummins, H. Z., Liquid, glass, gel: The phases of colloidal Laponite. *J. Non-Cryst. Solids* **2007,** *353*, 3891-3905.
50. Gaharwar, A. K.; Cross, L. M.; Peak, C. W.; Gold, K.; Carrow, J. K.; Brokesh, A.; Singh, K. A., 2D Nanoclay for Biomedical Applications: Regenerative Medicine, Therapeutic Delivery, and Additive Manufacturing. *Adv. Mater.* **2019,** *31*, 1900332.
51. U. Rojas Wahl, R.; Zeng, L.; A. Madison, S.; L. DePinto, R.; J. Shay, B., Mechanistic studies on the decomposition of water soluble azo-radical-initiators. *J. Chem. Soc., Perkin Trans. 2* **1998,** 2009-2018.
52. Ramos, J.; Forcada, J., Which are the mechanisms governing in cationic emulsion polymerization? *Eur. Polym. J.* **2007,** *43*, 4647-4661.
53. Noël, A.; Faucheu, J.; Chenal, J.-M.; Viricelle, J.-P.; Bourgeat-Lami, E., Electrical and mechanical percolation in graphene-latex nanocomposites. *Polymer* **2014,** *55*, 5140-5145.
54. Chenal, M.; Véchambre, C.; Chenal, J.-M.; Chazeau, L.; Humblot, V.; Bouteiller, L.; Creton, C.; Rieger, J., Mechanical properties of nanostructured films with an ultralow volume fraction of hard phase. *Polymer* **2017,** *109*, 187-196.
55. Chenal, M.; Rieger, J.; Véchambre, C.; Chenal, J.-M.; Chazeau, L.; Creton, C.; Bouteiller, L., Soft Nanostructured Films with an Ultra-Low Volume Fraction of Percolating Hard Phase. *Macromol. Rapid Commun.* **2013,** *34*, 1524-1529.
56. Veschambres, C.; Halma, M.; Bourgeat-Lami, E.; Chazeau, L.; Dalmas, F.; Prevot, V., Layered double hydroxides: Efficient fillers for waterborne nanocomposite films. *Appl. Clay Sci.* **2016,** *130*, 55-61.

For Table of Contents Only

Polymer/Laponite® nanocomposite films produced from surfactant-free latexes using cationic macroRAFT copolymers

Thaíssa C. Chaparro, Rodrigo D. Silva, Franck D'Agosto, Muriel Lansalot, Florent Dalmas, Laurent Chazeau, Amilton M. Santos*, Elodie Bourgeat-Lami*